Video Meteor Fluxes

M. D. Campbell-Brown • D. Braid

Keywords meteor · Eta Aquariid · sporadic · flux · video

1 Introduction

The flux of meteoroids, or number of meteoroids per unit area per unit time, is critical for calibrating models of meteoroid stream formation and for estimating the hazard to spacecraft from shower and sporadic meteors. Although observations of meteors in the millimetre to centimetre size range are common, flux measurements (particularly for sporadic meteors, which make up the majority of meteoroid flux) are less so. It is necessary to know the collecting area and collection time for a given set of observations, and to correct for observing biases and the sensitivity of the system.

Previous measurements of sporadic fluxes are summarized in Figure 1; the values are given as a total number of meteoroids striking the earth in one year to a given limiting mass. The Grün et al. (1985) flux model is included in the figure for reference. Fluxes for sporadic meteoroids impacting the Earth have been calculated for objects in the centimeter size range using Super-Schmidt observations (Hawkins & Upton, 1958); this study used about 300 meteors, and used only the physical area of overlap of the cameras at 90 km to calculate the flux, corrected for angular speed of meteors, since a large angular speed reduces the maximum brightness of the meteor on the film, and radiant elevation, which takes into account the geometric reduction in flux when the meteors are not perpendicular to the horizontal. They bring up corrections for both partial trails (which tends to increase the collecting area) and incomplete overlap at heights other than 90 km (which tends to decrease it) as effects that will affect the flux, but estimated that the two effects cancelled one another. Halliday et al. (1984) calculated the flux of meteorite-dropping fireballs with fragment masses greater than 50 g, over the physical area of sky accessible to the MORP fireball cameras, counting only observations in clear weather. In the micron size range, LDEF measurements of small craters on spacecraft have been used to estimate the flux (Love & Brownlee, 1993); here the physical area of the detector is well known, but the masses depend strongly on the unknown velocity distribution. In the same size range, Thomas & Netherway (1989) used the narrow-beam radar at Jindalee to calculate the flux of sporadics. In between these very large and very small sizes, a number of video and photographic observations were reduced by Ceplecha (2001). These fluxes were calculated (details are given in Ceplecha, 1988) taking the Halliday et al. (1984) MORP fireball fluxes, slightly corrected in mass, as a calibration, and adjusting the flux of small cameras to overlap with the number/mass relation from that work. Then faint video observations, which overlap with small cameras at their largest sizes, were similarly calibrated using the small camera data. The flux data from Ceplecha's study between 10^{-6} and 10^{-4} kg does not fit the slope between the LDEF and Super-Schmidt data (Figure 1), so uncertainty remains in this region. The flux in this size range is of particular importance, since much of the mass lost by comets is in particles of this size; also, the greatest danger to

M. D. Campbell-Brown (✉)
University of Western Ontario, London ON N6A 3K7 Canada. E-mail: margaret.campbell@uwo.ca

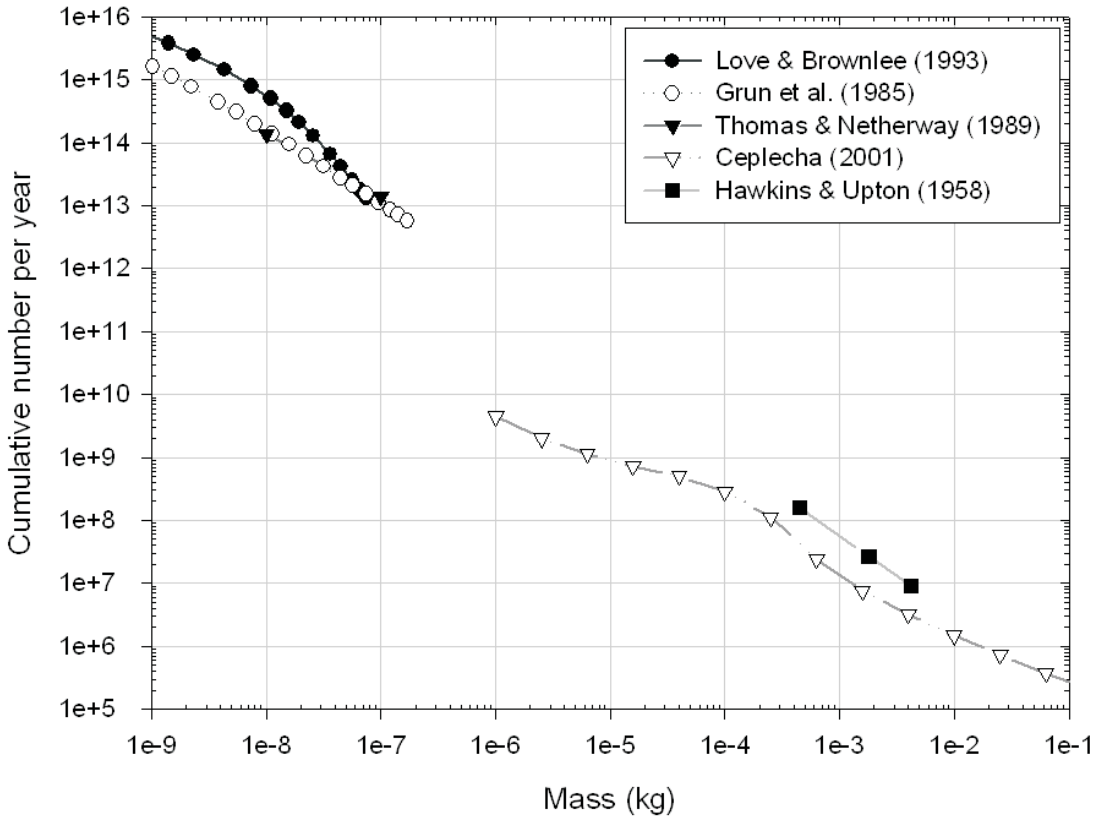

Figure. 1. Plot of meteoroid fluxes on the Earth from previous studies.

spacecraft comes from particles common enough to pose a real threat, and large enough to cause damage.

Shower fluxes have been estimated from visual observations (Brown & Rendtel, 1996), and from photographic and video observations. The usual method (employed in calculating Leonid fluxes by Koten et al. (2007), for example), uses the physical area observed by a pair of cameras at 100 km and applies a correction for radiant elevation. The most rigorous optical fluxes have been calculated for Leonids, Orionids and some minor showers (e.g. Gural et al., 2004; Trigo-Rodriguez et al., 2007, 2008) using a thorough simulation of the observing systems, including the camera sensitivity, range biases, and angular speed of the meteors on each camera. Details of the simulation are given in Molau et al. (2002).

In this work, we rigorously calculate the collecting area for a set of two intensified video cameras deployed in Arizona in 2006. The collecting area calculation was tested on the Eta Aquariid meteor shower and then applied to the antihelion, apex and north toroidal sporadic sources to obtain a sporadic flux.

2 Observations & Data Analysis

The data used in this study were taken from two sites in Arizona: the Fred Lawrence Whipple Observatory (31.675°N, 110.953°W) and Kitt Peak National Observatory (31.962°N, 111.60°W),using identical cameras, during a nine-night campaign in 2006. The baseline between the two sites was

approximately 75 km. Both systems had 25 mm, f/0.85 objective lenses, Gen III ITT image intensifiers, and Cohu 4910 video cameras. Each system produces 30 interlaced frames per second, with standard video resolution of 640×480 pixels and 8 bits per pixel. The data were recorded on digital tapes for later analysis. Two nights of data were analyzed for this project: April 27 and May 6, 2006. The latter is the peak of the eta Aquariid meteor shower.

The MeteorScan software package (Gural, 1997) was used to identify meteors in the data. A total of 235 meteors simultaneously observed with both cameras were identified. The astrometry and photometry were measured using an in-house software package called PhotoM. Trajectories of the two-station meteors were calculated using MILIG, developed by J. Borovička (Borovička, 1990). Photometric masses were calculated for each of the meteors, and the distribution of these masses was used to find the sporadic mass index, $s = 2.02 \pm 0.02$, and the limiting mass, 2.06×10^{-6} kg.

In order to calculate the flux of meteoroids from a particular radiant, the number of meteoroids must be counted. Rather than calculate a partial trail correction, we accept only meteors for which the maximum of the light curve occurred in the common volume of the two cameras. There is some uncertainty even in this strict criterion: many meteor light curves are nearly flat at the peak, so judging whether the maximum was just inside or just outside the volume can be difficult. Some meteors were growing fainter when they entered the field of view of both cameras, and some growing brighter as they left both cameras: while the first or last observed frame might have been the maximum, these meteors were excluded. This left 121 meteors in the sample.

Figure 2 shows the radiant distribution in ecliptic coordinates. The apex of the Earth's way is in the centre of the plot, and the antihelion source to the right, near the antihelion point at 180° ecliptic longitude. The antihelion source is the clearest feature: the north apex source is also identifiable. Although there are meteors in the region of the north toroidal source, its borders are not clearly defined. The Eta Aquariids are visible as a small cluster of radiants to the left of the apex source, just above the ecliptic around longitude 295°. There are virtually no meteors in the region of the south apex source, and only one close to the helion source. There are a large number of meteors which are not within the 15 degree radius of any of the sporadic sources.

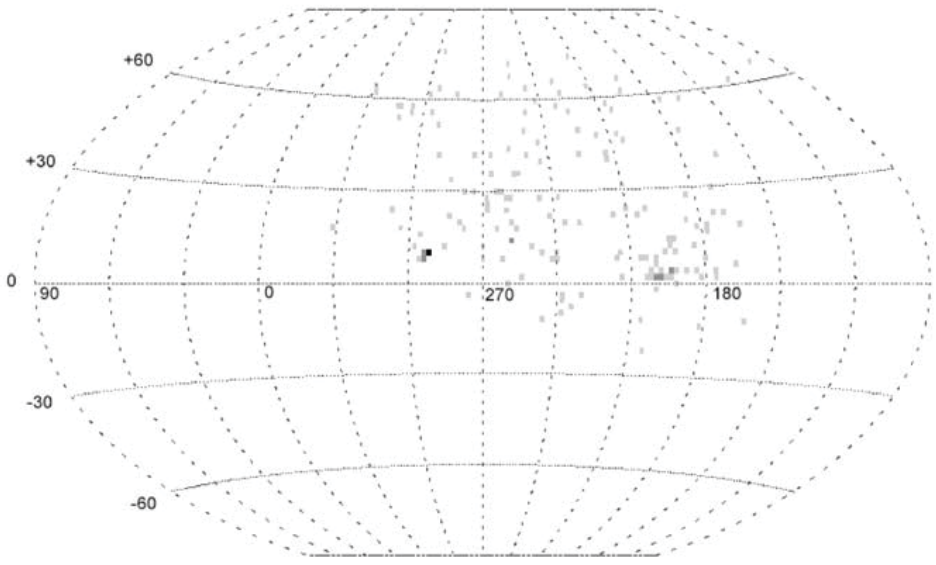

Figure 2. Radiants of meteors used in the flux study. The horizontal axis is the ecliptic plane; the apex of the Earth's way is in the centre (270° longitude) and the sun is at (0,0). The darkest dot represents six meteors with very close radiants; the lightest dots have only one meteor per 1 degree bin.

3 Collecting Area

If meteoroids all ablated at the same height, and detectors were uniformly sensitive, calculating the collecting area would be straightforward: the physical area covered by the detector at that height could be found quite simply. Even at a single height, the problem is more complicated: the sensitivity of a camera is generally a function of the position on the detector (with the most sensitivity generally occurring in the center of the field of view, and the least at the edges, mainly due to vignetting from the objective lens). The area in the sky is not at a uniform distance from the camera, so the limiting sensitivity will vary according to the range. Finally, the angular speed of the meteor as seen at the detector will influence whether or not it will be detected: a meteor coming straight at the camera may not be identified as a meteor at all, since it does not trace out a line, while one which is moving perpendicular to the line of sight will have its light in each frame spread over more pixels, which may reduce the signal until it is lost in the noise. All of these effects should properly be taken into account when calculating flux.

Even for shower meteors, the heights of meteors vary significantly from one to another, and meteors may not all cross one particular surface of constant height. In that case, the collecting area must be calculated at different heights, with a weighting for the probability of observing a meteor at that height.

The sensitivity of each camera was calculated from flatfields for each system. The optical centre of the image was found, using the highest pixel values in the flatfield to find the region of maximum sensitivity. The distance of each pixel in degrees from this optical centre was determined, and a fit performed to find the sensitivity as a fraction of the maximum as a function of angle from the centre.

For a particular radiant, the collecting area was calculated for half hour intervals throughout the night. For each time interval, slices from 80 to 120 km, with a spacing of 2 km, were taken; the corrected area of each slice was calculated, and a weighting factor was applied according to the height distribution of maximum luminosities of the meteors in the dataset. The weights, found using the distribution of maximum heights in the data set, were distributed as a Gaussian, with a maximum at 98 km and a standard deviation of 13 km; the final collecting area was normalized by dividing by the sum of the weights. Each slice was divided into squares 4 km × 4 km; the area of each square was weighted by the sensitivity of each camera, compared to the maximum sensitivity, the range to each camera squared, and the angular speed of a meteor from the given radiant at that position on each camera. If the trails at that point would be less than 3 pixels long, the area of that square was set to zero, assuming the meteor would not have been detected. The area was also weighted for the cosine of the zenith angle of the radiant, since the rate depends geometrically on the angle between the radiant and the surface. The total weighting factor was taken to the power of $s - 1$; if the mass index is large, there are many faint meteors, and more meteors will be missed in the less sensitive areas. If s is small, there are many bright meteors and fewer will be missed, so the collecting area is larger.

The integrated nightly collecting area for all heliocentric radiants is shown in Figure 3. It can be seen that the maximum collecting area occurs outside the sporadic sources, and partly explains the large number of meteors observed outside the sources. The collecting area for the north apex and antihelion sources are actually low compared to other parts of the sky. The region where the radiants pass through the fields of view of the cameras is also clearly visible as a cuved line of lower collecting areas in the middle of the maximum area.

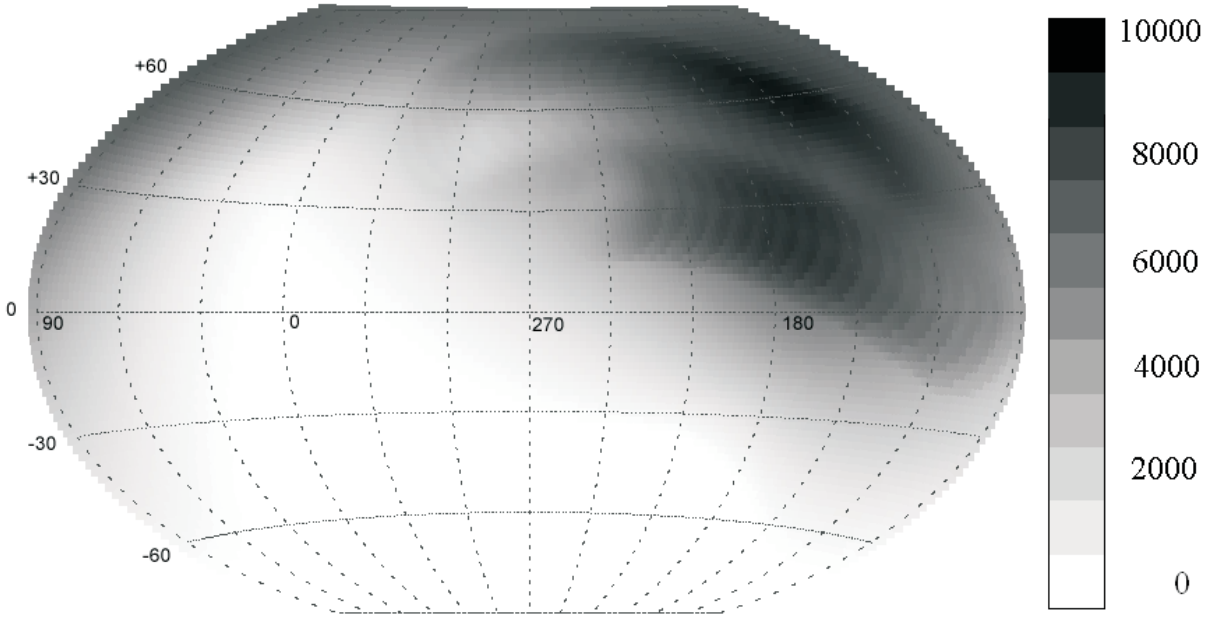

Figure 3. Integrated daily collecting area of the video system in heliocentric coordinates (as in Figure 2).

4 Eta Aquariid Fluxes

May 6, 2006 was the peak of the Eta Aquariid meteor shower. Although the radiant rose only about two hours before dawn at the observing site, and only 8 two-station Eta Aquariids had their light curve maximum in the common volume, we calculated the shower flux as a test of the method. The IMO value of the mass index, 1.95, was used (Dubietis, 2003), even though this is for larger visual meteoroids, since there were not enough Eta Aquariid meteors in our sample to calculate the mass index. The collecting area of the system for the Eta Aquariid radiant is shown in Figure 4.

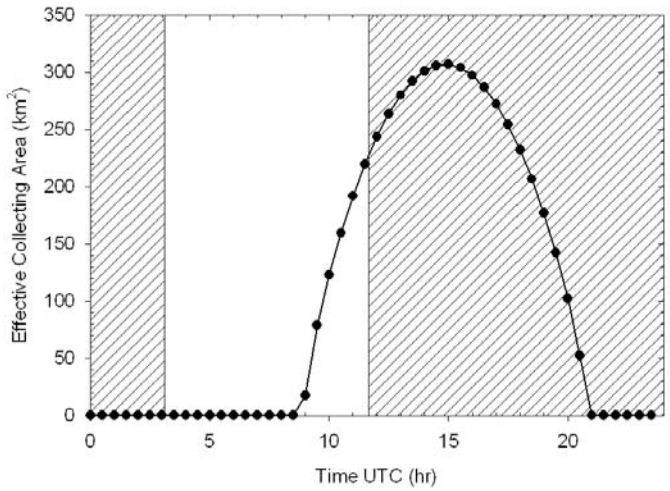

Figure 4. Collecting area for the Eta Aquariid radiant at half-hour intervals. The shaded regions indicate times when the sky was too bright to observe, starting and ending at nautical twilight.

The non-zero collecting areas were summed and the flux obtained for the two hour period was 0.0028 ± 0.0009 meteoroids km^{-2} hr^{-1}. This corresponds to a zenithal hourly rate of 65 (see Brown & Rendtel, 1996, for the formula to convert between ZHR and flux), which is very close to the value recorded for visual observations that year by the IMO (imo.net). This is certainly due partly to chance; since the number of meteors used in the flux calculation was so small, there are significant uncertainties in the estimate, but it gives us confidence that the collecting area calculation is correct.

5 Sporadic Fluxes

Sporadic fluxes are slightly more complicated than shower fluxes. The sources are diffuse, so the radius chosen will strongly affect the number of echoes included and therefore the flux. The collecting area also varies significantly across the source: the leading edge of the source can rise more than an hour before the trailing edge. When calculating the angular speed, there are uncertainties not only because of the large radiant area, but also because the speeds of the meteors have a broad distribution around the average, instead of being tightly confined as shower speeds are. For this study, we take a simple approach. Each source is divided into four quadrants, and the collecting area for each quadrant is calculated in half hour intervals. The average of these four values is used as the true collecting area. This approach is more efficient than the more rigorous version, which would involve calculating the collecting area for dozens of points around the source and then performing a weighted average reflecting the differing activity of each small point around the source, and it correctly reproduces the slow rise in collecting area as the radiant moves above the horizon. In calculating angular velocity, the average speed for each source (30 km/s for the antihelion, 35 km/s for the north toroidal, and 60 km/s for the north toroidal) was used rather than a distribution. The collecting area should be slightly lower for meteors moving faster than the average, and slightly higher for slower meteors, but the total collecting area should be the same if the velocity distributions are Gaussian.

Fluxes were calculated separately for the two nights of data, since the collecting areas for each source vary very slightly in that time period. Since the number of observed meteors was low, hourly fluxes were not calculated; the total number of meteors from each source was divided by the average collecting area. It was not possible to calculate a mass index for each source individually from the small numbers, so a mass index of 2.0 was assumed for each source, consistent with the *s* measured for all the sporadics observed in the dataset.

A total of 24 antihelion, 21 north apex, and 15 north toroidal meteors were recorded on the two nights. When divided by collecting area (pictured in Figures 5-7), this produced fluxes of 0.039 ± 0.006 meteoroids km^{-2} hr^{-1} for the antihelion source, 0.041 ± 0.006 meteoroids km^{-2} hr^{-1} for the north apex, and 0.012 ± 0.002 meteoroids km^{-2} hr^{-1} for the north toroidal. The errors were calculated using Poisson statistics for the small numbers, plus estimates of the error due to assuming a mass index and height distribution based on small numbers. The collecting area was varied to look at a reasonable range of mass indices for each source, and was found to vary by about 10%. The change in the weighted area of a slice from 90 km to 110 km was also found to be close to 10%.

To find the total sporadic flux, the flux from each of the three observed sources was doubled to account for its unobserved pair: the helion, south apex and south toroidal sources. This ignores the fact that the flux of the helion and antihelion sources vary through the year and the maxima and minima do not coincide (Campbell-Brown & Jones, 2006). It is believed that the pairs of sources have very close to symmetrical flux values when summed over the year, so this method should give a good annual value if there was more data. We proceed with this value, knowing that it is based on too little data, to see how it compares to previous studies.

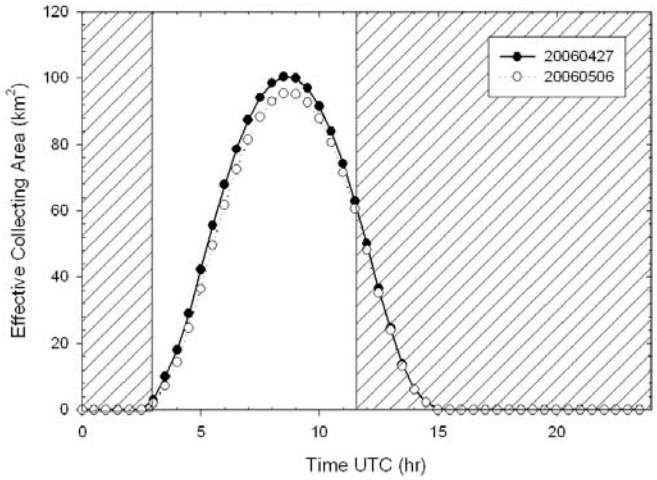

Figure 5. Collecting area for the antihelion source. The shaded regions indicate daytime until nautical twilight, when the sky was too bright to observe.

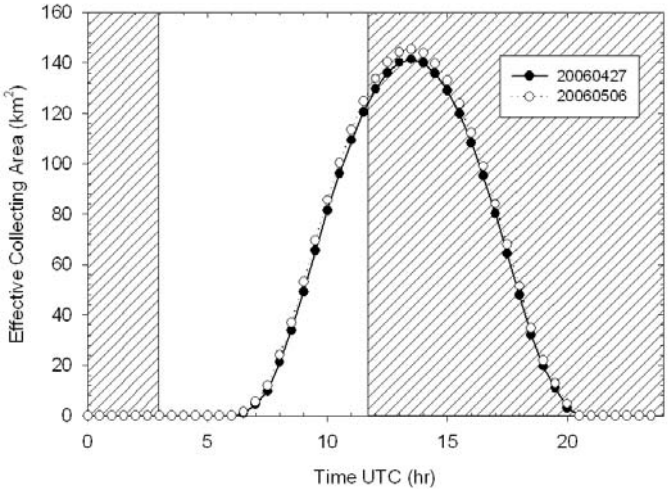

Figure 6. Collecting area for the north apex source.

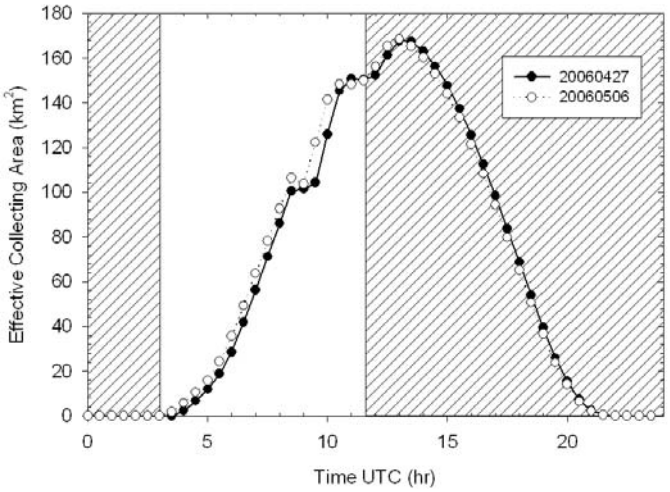

Figure 7. Collecting area for the north toroidal source.

The total sporadic flux from all the sources is 0.18 ± 0.04 meteoroids km^{-2} hr^{-1}. To compare this to the studies mentioned in the introduction, we convert this to a fluence over the whole Earth over a year, by multiplying by the cross-sectional area of the Earth and the number of hours in a year. The total is $(2.0 \pm 0.4) \times 10^{11}$ meteoroids.

The error bars include only errors in our measured value: they do not reflect the fact that the sporadic flux changes over the course of a year and that figures for part of two days are being used to estimate the flux over a full year. Figure 8 shows this result with previous studies. Note that the error bars are smaller than the symbol, because of the logarithmic scale.

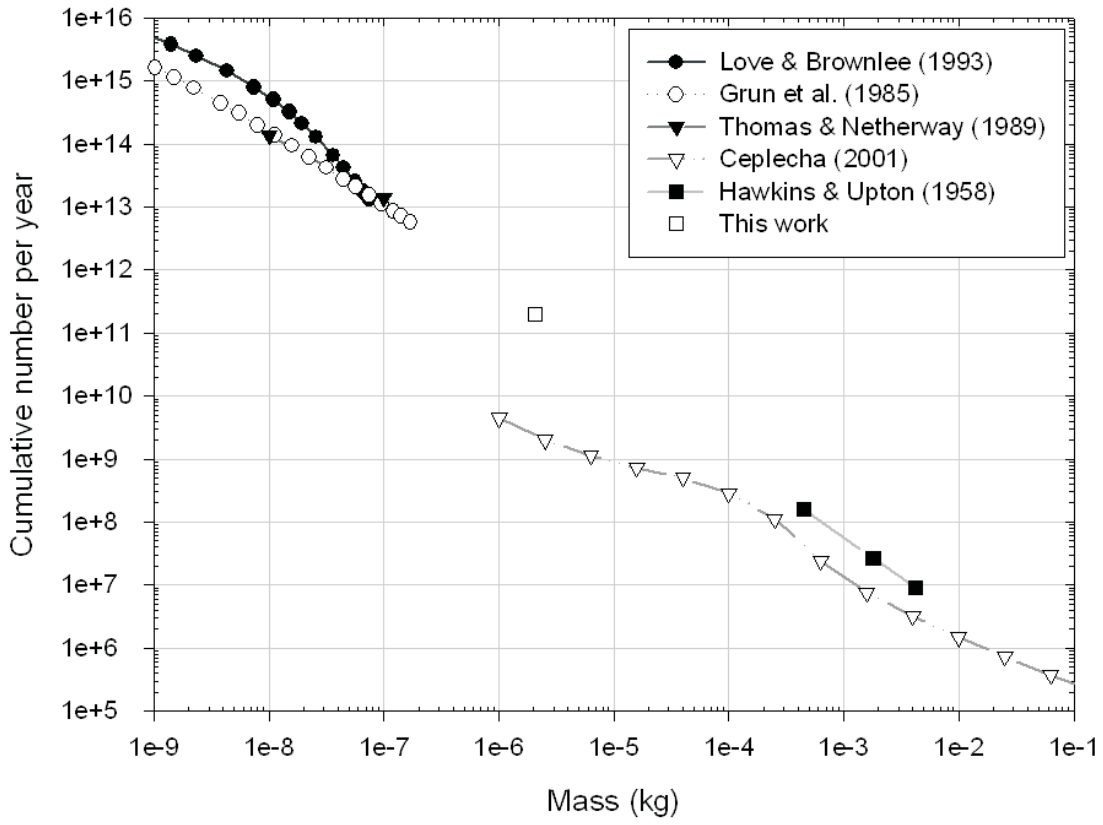

Figure 8. Plot of meteoroid fluxes on the Earth from previous studies, with the data point from the current study.

6 Discussion

The flux results for the Eta Aquariid meteor shower, though based on few meteors, are very promising, and give confidence that our method of calculating collecting area for particular radiants gives reasonable results. Shower fluxes are easier to calculate than sporadic fluxes, because of the higher numbers and narrow range of radiants and velocities, and more measurements with other systems are available for comparison, so future studies will examine more showers to further validate the method.

The total sporadic flux measured in this study fits surprisingly well on a line joining the fireball camera data to the Grün model, and is well above the flux from video studies by Ceplecha (2001). The fit is more surprising considering that it is based on only two nights of data from one part of the year, and a total of only 60 meteors.

The flux reported here reflects only meteoroids with radiants in one of three sporadic sources. An additional 61 meteors with maximum luminosity in the common volume were not included in the flux calculations because their radiants lay outside the sources. While this would seem to introduce a factor of two error in our measurement, we believe that the actual change in flux would be small if these other meteors were included. Inspection of Figures 2 and 3 shows that most of the meteors from radiants outside the sources occur in regions of the sky with very large collecting areas, meaning that the flux from those areas will be low.

For the past year, we have been running an automated two-station video system at the University of Western Ontario, and have collected over 1500 two-station meteor observations, mostly sporadic meteors. This dataset will be the subject of the next flux study, which will use a much larger dataset collected over a much more extensive range of solar longitudes to calculate the flux of sporadic meteors. In addition to the flux from the sporadic sources, this new study will calculate the fluxes from the whole visible sky, something which will be possible with much larger numbers. This new flux value, and the mass index which will accompany it, will better fill in the gap in our understanding of meteoroids in the millimetre to centimetre size range.

Acknowledgements

Thanks to Jean-Baptiste Kikwaya and Shannon Nudds, who collected the video data, and to the NASA Meteoroid Environment Office for funding.

References

Borovička J., “The Comparison of Two Methods of Determining Meteor Trajectories from Photographs”, Astronomical Institutes of Czechoslovakia, Bulletin 41, 391-396 (1990)

Brown P., Rendtel J., “The Perseid Meteoroid Stream: Characterization of recent activity from visual observations”, Icarus, 124, 414-428 (1996)

Campbell-Brown M., Jones J., “Annual Variation of Sporadic Radar Meteor Rates”, MNRAS 367, 709-716 (2006)

Ceplecha Z., “Earth's Influx of Different Populations of Sporadic Meteoroids from Photographic and Television Data”, BAICz 39, 221-236 (1988)

Ceplecha Z., “The Meteoroidal Influx to the Earth”, in Collisional Processes in the Solar System, 35-50. Kluwer, Dordrecht (2001)

Dubietis A., “Long-term Activity of Meteor Showers from Comet 1P/Halley”, JIMO 31, 43-48 (2003)

Halliday I., Blackewell A.T., Griffin A.A., “The frequency of meteorite falls on the earth”, Science 223, 1405-1407 (1984)

Hawkins G., Upton E., “The Influx Rate of Meteors in the Earth's Atmosphere”, ApJ, 128, 727-735 (1958)

Grün E., Zook H.A., Fechtig H., Geise R.H., “Collisional Balance of the Meteoritic Complex”, Icarus 62, 244-272 (1985)

Gural P., “An Operational Autonomous Meteor Detector: Development Issues and Early Results”, JIMO 25, 136-140 (1997)

Gural P., Jenniskens P., Koop M., Jones M., Houston-Jones J., Holman D., Richardson J. “The Relative Activity of the 2001 Leonid Storm Peaks and Implications for the 2002 Return”, AdSpR 33, 1501-1506 (2004)

Koten P., Borovička J., Spurny P., Evans S., Štork R., Elliott A., “Video Observations of the 2006 Leonid Outburst”, EM&P 102, 151-156 (2007)

Love S., Brownlee D., “A Direct Measurement of the Terrestrial Mass Accretion Rate of Cosmic Dust”, Science, 262, 550-553 (1993)

Molau S., Gural P., Okamura O., “Comparison of the `American' and the `Asian' 2001 Leonid Meteor Storm”, JIMO 30, 3-21 (2002)

Thomas R.M., Netherway D.J., “Observations of Meteors Using an Over-the-horizon Radar”, PASAu 8, 88-93 (1989)

Trigo-Rodriguez J., Madiedo J., Llorca J., Gural P., Pujols P., Tezel T., “The 2006 Orionid Outburst Imaged by All-sky CCD Cameras from Spain: Meteoroid spatial fluxes and orbital elements”, MNRAS 380, 126-132 (2007)

Trigo-Rodriguez J., Madiedo J., Gural P., Castro-Tirado A., Llorca J., Fabregat J., Vitek S., Pujols P., “Determination of Meteoroid Orbits and Spatial Fluxes by Using High-Resolution All-Sky CCD Cameras”, EM&P 102, 231-240 (2008)